Fibril Paint: a class of amyloid-targeting peptides

Júlia Aragonès Pedrola[a,b,c,*], Françoise A. Dekker[a,b,c,*], Katrin Guttmann[c,@], Litske M. van Leeuwen[b,c,@], Shalini Singh[d], Guy Mayer[d], Tommaso Garfagnini[d], Assaf Friedler[d,#], Stefan G. D. Rüdiger[a,b,c,#]

Neurodegenerative diseases, such as Alzheimer's Disease, Parkinson's Disease and Huntington's Disease, are characterised by accumulation of amyloid fibrils, which remain incurable. It is of great importance to develop early-diagnosis approaches as well as disease-modifying therapies. Recently, we discovered the FibrilPaint1 peptide, a specific amyloid binder that can serve for fibril diagnosis. Here we introduce a class of FibrilPaint1 derivatives that bind to protein fibrils. The modifications include variation of the charge, termini and order of residues. As a result, we generated a class of peptides with general fibril-binding properties and with the potential for further adaptation, such as linkage to multiple dyes, optimisation for specific protein and aggregate strains, or adaptation for targeted protein degradation strategies. Thus, Fibril Paint peptides are a class of promising leads for targeting amyloid fibrils for diagnostic and therapeutic purposes.

Introduction

Protein aggregation into amyloid fibrils characterizes the development of neurodegenerative diseases[1, 2], such as Alzheimer's Disease (AD), Parkinson's Disease (PD) and Huntington's Disease (HD). These disorders are defined by the gradual deterioration of brain function, followed by cognitive and motor impairments.

To date, neurodegenerative diseases remain incurable. The underlying mechanism is poorly known, precluding systematic development of causal treatments. Recently, Lecanemab, a monoclonal antibody clearing Aβ plaques[3-5], has been approved by the FDA. However, given the potentially severe side effects, the EMA refused approval in the EU as the benefits do not outweigh the risks[6]. An important factor to increase effectivity of these treatments is administration at early stages of the disease[5], which again requires early diagnosis. Taken together, these facts strengthen the need for developing early-diagnosis and disease monitoring approaches, as well as disease modifying therapies.

Recently, as an intersection of rational design for aggregation preventors[7] and characterisation fibril interactome[8] we discovered FibrilPaint1 (FP1)[9]. FP1 is a fluorescently labelled, 22-residues peptide that specifically binds various disease-relevant protein fibrils at nanomolar affinity. These fibrils include early stages from recombinant Tau, Huntingtin (Htt), α-synuclein and Amyloid-β, and patient-derived fibrils from AD, Frontotemporal Dementia and Corticobasal Degeneration. The binding capacity of FP1 is hypothesised to be due to its enriched sequence in aromatic and π-stacking residues that are also capable of extended H-bonding, but the molecular signature remains unknown.

In the context of neurodegenerative disease therapies and diagnosis, there is the need for variation of FP1. Modifications in the sequence of this peptide can lead to improved binding, adaptation of the dye according to desired imaging technique, adjustment of the charge for drug delivery, or modification of the termini to develop targeted degradation strategies. Here we show that various Fibril Paint peptides resulting from the systematic modification of the FP1 sequence bind to Tau and Htt fibrils. As a result, we have developed a new class of amyloid-targeting peptides, which broaden the basis for the development of compounds targeting amyloid fibrils.

Methods

Peptide synthesis and purification

The peptides were synthesized using a Liberty Blue Microwave-Assisted Peptide Synthesizer (CEM) with standard Fmoc chemistry and DIC/Oxyma as coupling reagents. The peptide concentrations were measured by UV spectroscopy. The peptides were labelled with 5(6)-carboxyfluorescein at their N' termini[10]. The peptides were cleaved from the resin with a mixture of 95 % (v/v) trifluoroacetic acid (TFA), 2.5% (v/v) triisopropylsilane (TIS), 2.5 % (v/v) triple distilled water (TDW) agitating vigorously for 3 hours at room temperature. The volume was decreased by N_2 flux, and the peptides precipitated by addition of 4 volumes of diethylether at -20 °C. The peptides were sedimented at -20 °C for 30 minutes, then centrifuged and the diethylether discarded. The peptides were washed three times with diethylether and dried by gentle N_2 flux. The solid was dissolved in 1:2 volume ratio of acetonitrile (ACN):TDW, frozen in liquid Nitrogen and lyophilized. The peptides were purified on a WATERS HPLC using a reverse-phase C18 preparative column with a gradient ACN/TDW. The identity and purity of the peptides was verified by ESI mass spectrometry and Merck Hitachi analytical HPLC using a reverse-phase C8 analytical column.

Expression and purification of TauRD

We produced N-terminally FLAG-tagged (DYKDDDDK) human TauRD (Q244-E372, with pro-aggregation mutation ΔK280) in *E. Coli* BL21 Rosetta 2 (Novagen), with an additional removable N-terminal His_6-Smt-tag (MGHHHHHHGSDSEVNQEAKPEVKPEVKPETHINLKVSDGSSEIFFKIKKTT

[a] Cellular Protein Chemistry, Bijvoet Center for Biomolecular Research, Utrecht University, Padualaan 8, 3584CH Utrecht, The Netherlands.
[b] Science for Life, Utrecht University, Padualaan 8, 3584CH Utrecht, The Netherlands.
[c] Protein Chemistry of Disease, Department of Chemistry, Utrecht University, Padualaan 8, 3584CH Utrecht, The Netherlands
[d] Institute of Chemistry, The Hebrew University of Jerusalem, Edmond J. Safra Campus at Givat Ram, Jerusalem 9190401, Israel
* These authors contributed equally
@ These authors contributed equally
# Corresponding authors

PLRRLMEAFAKRQGKEMDSLRFLYDGIRIQADQTPEDLDMEDNDIIEAHRE QIGG). Expression was induced at OD600 0.8 by addition of 0.15 mM IPTG and incubation at 18 °C overnight. Cells were harvested by centrifugation, resuspended in 25 mM HEPES-KOH pH=8.5, 50 mM KCl, flash frozen in liquid nitrogen, and kept at – 80 °C until further usage. Pellets were thawed at 37 °C, followed by the addition of ½ tablet/50 ml EDTA-free Protease Inhibitor and 5 mM β-mercaptoethanol. Cells were disrupted using an EmulsiFlex-C5 cell disruptor, and lysate was cleared by centrifugation. Supernatant was filtered using a 0.22 µm polypropylene filtered and purified with an ÄKTA purifier chromatography System. Sample was loaded into a POROS 20MC affinity purification column with 50 mM HEPES-KOH pH 8.5, 50 mM KCl, eluted with a linear gradient 0-100%, 5 CV of 0.5 M imidazole. Fractions of interest were collected, concentrated to 2.5 ml using a buffer concentration column (vivaspin, MWCO 10 KDa), and desalted using PD-10 desalting column to HEPES pH 8.5, ½ tablet/50 ml Complete protease inhibitor, 5 mM β-mercaptoethanol. The His_6-Smt-tag was removed by treating the sample with Ulp1, 4 °C, shaking, overnight. The next day, sample was loaded into POROS 20HS column with HEPES pH 8.5, eluted with 0-100% linear gradient, 12 CV of 1M KCl. Fractions of interest were collected and loaded into a Superdex 26/60, 200 pg size exclusion column with 25 mM HEPES-KOH pH 7.5, 75 mM NaCl, 75 mM KCl. Fractions of interest were concentrated using a concentrator (vivaspin, MWCO 5 kKDda) to desired concentration. Protein concentration was measured using a NanoDrop™ OneC UV/Vis spectrophotometer and purity was assessed by SDS-PAGE. Protein was aliquoted and stored at – 80 °C.

Expression and purification of HttEx1Q44

We produced HttEx1Q44 with in *E. Coli* BL21 Rosetta 2 (Novagen), with an additional N-terminal MBP- and C-terminal His_6-tag (MKIEEGKLVIWINGDKGYNGLAEVGKKFEKDTGIKVTVEHPDKLEEKFPQV AATGDGPDIIFWAHDRFGGYAQSGLLAEITPDKAFQDKLYPFTWDAVRYN GKLIAYPIAVEALSLIYNKDLLPNPPKTWEEIPALDKELKAKGKSALMFNLQEP YFTWPLIAADGGYAFKYENGKYDIKDVGVDNAGAKAGLTFLVDLIKNKHM NADTDYSIAEAAFNKGETAMTINGPWAWSNIDTSKVNYGVTVLPTFKGQP SKPFVGVLSAGINAASPNKELAKEFLENYLLTDEGLEAVNKDKPLGAVALKSY EEELAKDPRIAATMENAQKGEIMPNIPQMSAFWYAVRTAVINAASGRQTV DAALAAAQTNAAAASEFSSNNNNNNNNNLGIEGRMATLEKLMKAFESL KSFQQQQQQQQQQQQQQQQQQQQQQQQQQQQQQQQQQQQQQQQQ QQQQQPPPPPPPPPPQLPQPPPQAQPLLPQPQPPPPPPPPPGPAVAEE PLHRPSGSHHHHHH). We induced expression at an OD600 of 0.8 by adding 0.15 mM IPTG and incubating at 18 °C overnight. Cells were harvested by centrifugation and resuspended in 50 mM HEPES-KOH pH=8.5, 50 mM KCl with ½ tablet/50 ml EDTA-free Protease Inhibitor and 5 mM β-mercaptoethanol. Cells were disrupted using an EmulsiFlex-C5 cell disruptor, and lysate was cleared by centrifugation. Supernatant was filtered using a 0.22 µm polypropylene filtered and purified with an ÄKTA purifier chromatography System. Sample was loaded into a POROS 20MC affinity purification column with 50 mM HEPES-KOH pH 8.5, 100 mM KCl, eluted with a linear gradient 0-100%, 10 CV of 0.5 M imidazole, 30 mM NaCl. Fractions of interest were collected, buffer exchanged to 50 mM HEPES 150 mM NaCl and concentrated to desired concentration using a Vivaspin column (vivaspin, MWCO 30 KDa). Protein concentration was measured using a NanoDrop™ OneC UV/Vis spectrophotometer and purity was assessed by SDS-PAGE. Protein was aliquoted and stored at – 80 °C.

TauRD fibril formation

Aggregation of 20 µM TauRD in 25 mM HEPES-KOH pH 7.4, 75 mM KCl, 75 mM NaCl, ½ tablet/50 ml Protease Inhibitor, was induced by the addition 5 µM of heparin low molecular weight and incubated at 37 °C and 600 rpm in an Eppendorf™ Thermomixer® during 20 hours. Fibrils were made independently, per measurement.

HttEx1Q44 fibril formation

Aggregation of 20 µM HttEx1Q44 in 25 mM HEPES-KOH pH 7.4, 75 mM KCl, 75 mM NaCl, ½ tablet/50 ml Protease Inhibitor, was induced by the cleavage of C-terminal MBP-tag with Factor Xa and incubated at 37 °C and 600 rpm in an Eppendorf™ Thermomixer® during 5 hours. Fibrils were made independently, per measurement.

Size measurement with Flow Induced Dispersion Analysis

200 nM of Fibril Paint was measured in presence or absence of 2 µM preformed TauRD or HttEx1Q44 fibrils in 25 mM HEPES-KOH pH 7.5, 75 mM KCl, 75 mM NaCl, 0.5% pluronic (for TauRD) or 50 mM HEPES-KOH pH 7.5, 150 mM KCl, 0.5% pluronic (for HttExQ44). Size measurements were performed in a FIDA1 instrument with a 480 nm excitation source, using a capillary dissociation (Capdis) approach. In this, the capillary is equilibrated with buffer followed by injection of the sample.

Table 1. Experimental parameters for analysis of proteins up to R_h of 10 nm

Tray	Vial	Pressure (mbar)	Time (s)	Outlet	Measure	Comments
2	1	3500	45	Variable	No	1 M NaOH
2	2	3500	75	Variable	No	Buffer equilibration
1	Analyte	3500	20	Variable	No	Buffer
1	Indicator	50	10	Variable	No	Sample application
1	Analyte	400	180	Variable	Yes	Buffer
Tray 1 was maintained at 37 °C and tray 2 and capillary chamber at 25 °C						

Table 2. Experimental parameters for analysis of proteins up to R_h of 75 nm

Tray	Vial	Pressure (mbar)	Time (s)	Outlet	Measure	Comments
2	1	3500	45	Variable	No	1 M NaOH
2	2	3500	75	Variable	No	Buffer equilibration
1	Analyte	3500	20	Variable	No	Buffer
1	Indicator	50	10	Variable	No	Sample application
1	Analyte	75	1800	Variable	Yes	Buffer
Tray 1 was maintained at 37 °C and tray 2 and capillary chamber at 25 °C						

Results

Design and development of a new class of amyloid-targeting peptides

Recently we discovered FP1[9], a peptide binding to multiple amyloid fibrils, but not the monomeric precursors. FP1 consists of a fluorescein group (Fl), an amyloid-binding motif (PWWRRPWWPWHHPH), a linker (GSGS) and an E3-binding motif (EEVD) (Fig. 1). The EEVD is a recruiter of the E3 ligase CHIP, for targeted protein degradation. In contrast, the FP1 derivatives FP2, FP3 and FP4 (PWIRRPWWPWTTPTGSGSEEVD, PWWDDPWWPWTTPTGSGSEEVD, and PWWDDPWWPWHHPHGSGSEEVD) did not bind effectively to fibrils. They differ from FP1 in the amyloid-binding motif, which apparently decreases their affinity to amyloid fibrils.

Here we set out to search for FP1 derivatives that can maintain fibril-binding properties (Fig. 1, Table 3). For FP5, we removed the linker and E3 binding motif and added an extra positive charge. In FP6, the linker and E3 binding motif were removed. In FP7, the E3 binding motif was modified adding two extra positive charges. FP8 has an additional positive charge and a randomization of the sequence. FP9, FP10 and FP11 have the amyloid binding site of FP2, FP3 and FP4, respectively, and an additional positive charge. FP12 has an additional positive charge, and an amyloid binding motif composed of D-amino acids. FP13 has an additional positive charge and Arg, Pro and His residues are incorporated in D-form. Altogether, the modifications include shortening of the sequence to exclude the linker and E3 binding motif (FP5 and FP6), change of the net charge (FP5-FP13), randomisation of the sequence (FP8) and alteration of the 3D structure and increasing peptide stability using D-amino acids (FP12 and FP13).

Figure 1. Fibril Paint peptides. Schematical representation of Fibril Paint peptides used in this study. D-amino acids are referred as lower-case letters. Fl indicates the presence of a fluorescein group.

Various Fibril Paints target amyloids

Next, we aimed to determine the binding capacity of the FP peptides to amyloid fibrils. To do so, we used Flow Induced Dispersion Analysis (FIDA). FIDA is an established microfluidics and ensemble method, in which fluorescently labelled molecules disperse in solution[11, 12]. As a read-out it provides the Hydrodynamic Radius (R_h) which is a measure for the apparent mean size of a biomolecular complex in solution. In addition, based on the structure, we have developed an application to precisely determine the length of the fibrils[9]. FP peptides alone, which are fluorescently labelled, have a predicted R_h ranging from 1.03 nm to 1.17 nm (Table 3). If FP binds to the fibrils, the measured size will increase. Consequently, we can assess binding of FP peptides to fibrils, as well as determine their length.

To test the capacity of FP to bind amyloid fibrils, we used TauRD and HttEx1Q44 as model fibrils. Formation of Tau fibrils is associated with the development of AD[13], and Htt fibrilization is related to the progression of HD[14]. These two proteins differ in sequence and structure, and the only characteristic they share is the ability to form amyloid fibrils.

Following that approach, five FP peptides increased size in presence of TauRD fibrils grown for 20 hours and HttEx1Q44 fibrils grown for 5 hours (Fig 2., Table 3). Specifically, the R_h measured for TauRD fibrils together for five active FP peptides (FP1, FP5, FP6, FP7 and FP8) increased to an average size of 37 nm. In case of HttEx1Q44, we observed an average R_h of 198 nm (FP1, FP5, FP6 and FP7; the value for FP8 was not determined). The fibril size variation within the measurement using different FPs is minimal and does not depend on the FP. Given that the aggregation process is a seeded event, it is expected to observe some variation in the measured R_h. Together, these results indicate that FP1, FP5, FP6, FP7 and FP8 are effective fibril binders.

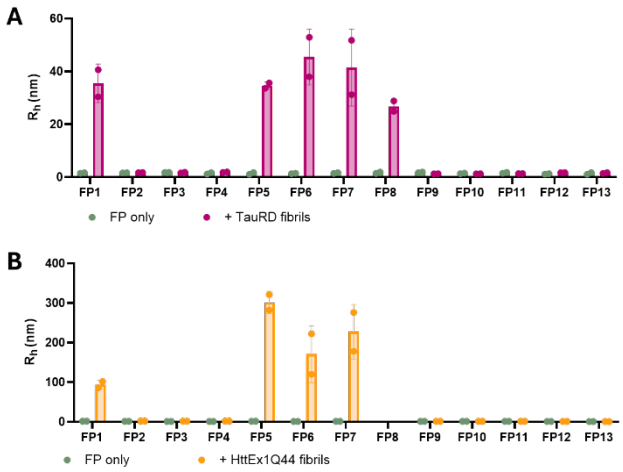

Figure 2. Fibril Paint peptides binding to fibrils. Fibril Paint binding to TauRD (A) or HttEx1Q44 (B) fibrils. Fibril Paint peptides alone are shown in green, in the presence of TauRD fibrils in pink, in the presence of HttEx1Q44 fibrils in orange (FP8: not determined).

Table 3. Properties of Fibril Paint peptides. (Fl) indicates Fluorescein group. Amino acids are coloured as large hydrophobic/aromatic, yellow; negative charge, red; positive charge, blue. D-amino acids are referred as lower-case letters. Predicted R_h is the expected hydrodynamic radius based on the size of the peptide. The binding is assessed by the ability to measure the size of fibrils in a FIDA experiment. Peptides that show activity are listed on top.

Name	Sequence	Predicted R_h (nm)	R_h (nm)		Binding	
			Tau	Htt	Tau	Htt
FibrilPaint1	(Fl)-PWWRRPWWPWHHPHGSGSEEVD	1.15	35.50	94.10	Yes	Yes
FibrilPaint5	(Fl)-PWWRRPWWPWHHPHR	1.06	34.64	301.50	Yes	Yes
FibrilPaint6	(Fl)-PWWRRPWWPWHHPH	1.04	45.45	171.00	Yes	Yes
FibrilPaint7	(Fl)-PWWRRPWWPWHHPHGSGSRRVD	1.16	41.49	227.00	Yes	Yes
FibrilPaint8	(Fl)-WWHPEPPHVRSWSWWRHGRGED	1.16	26.84	n.d.	Yes	n.d.
FibrilPaint2	(Fl)-PWIRRPWWPWTTPTGSGSEEVD	1.13	1.68	2.00	No	No
FibrilPaint3	(Fl)-PWWDDPWWPWTTPTGSGSEEVD	1.13	1.53	1.80	No	No
FibrilPaint4	(Fl)-PWWDDPWWPWHHPHGSGSEEVD	1.14	1.82	2.25	No	No
FibrilPaint9	(Fl)-PWIRRPWWPWTTPTR	1.03	1.25	1.50	No	No
FibrilPaint10	(Fl)-PWWDDPWWPWTTPTD	1.03	1.33	1.45	No	No
FibrilPaint11	(Fl)-PWWDDPWWPWHHPHD	1.04	1.37	1.44	No	No
FibrilPaint12	(Fl)-pwwrrpwwpwhhphrGSGSEEVD	1.17	1.68	1.14	No	No
FibrilPaint13	(Fl)-pWWrrpWWpWhhphrGSGSEEVD	1.17	1.70	1.69	No	No

The sequence of Fibril Paint peptides can be modified while retaining activity

The identification of four new FP peptides binding amyloid fibrils (FP5, FP6, PF7 and FP8) demonstrates that the sequence of FP1 can be varied while maintaining specific recognition of amyloid fibrils. First, the change in charge does not compromise binding ability. FP1 has a net charge of -1, and FP5, FP6, FP7 and FP8 have a net charge of +3, +2, +2, and 0, respectively. FP5 and FP6 lack the GSGS and the EEVD motifs, and in FP7 EEVD has been replaced by RRVD, indicating that those motifs are not required for detection of amyloid fibrils. In FP8, the order of the amino acid sequence is altered, indicating a potential to vary the sequential order of the residues.

In contrast, FP9, FP10, FP11, FP12 and FP13 lost ability to bind fibrils, suggesting that some components of the sequence are important to preserve the binding capacity. R and H seem to have an essential role, since the loss of these residues compromised the binding capacity of FP9, FP10 and FP11. Remarkably, the backbone conformation is important, considering that FP12 and FP13, which have D-amino acids, do not detect amyloid fibrils in FIDA measurements.

Discussion

Here, we developed a class of peptides, named Fibril Paint, that specifically target amyloid fibrils. These peptides are derivatives of FP1, which we previously discovered as a specific amyloid binder. In this study, we identified four new peptides binding amyloids: FP5, FP6, FP7 and FP8. Those peptides tolerated certain modifications without losing functionality, like variation of the charge, variation or removal of the terminus and rearrangement of residues order. These results are consistent with previous findings. Although the changes of FP5, FP6, FP7 and FP8 varied, the total amount of arginine residues was constant, suggesting that arginine may play a key role in the recognition of amyloid Tau that relies on π-stacking and H-bonding, not on charge[8]. The removal or alteration of both linker and terminus is not expected to affect the fibril binding capabilities of FP, as the GSGSEEVD sequence does not exert amyloid recognition. Finally, the conservation of the amyloid binding capabilities upon rearrangement is consistent with the recent report that molecular determinants, and not a specific sequence, confer inherent anti-aggregation properties to a peptide[7].

In the context of drug development, targeted protein degradation has become a promising strategy for removal of amyloid fibrils[15-19]. FP peptides are heterobifunctional compounds that can be used with that purpose. The EEVD motif in the C-terminus is a recruiter of that E3 ligase CHIP[20]. The formation of a ternary complex with the fibrils, can lead to their ubiquitination and subsequent degradation. Our data here show that EEVD motif can be modified, meaning that it can be adapted to recruit other E3 ligases, and change nature of targeted degradation, for instance autophagy[21-24]. Another important aspect is the modulation of the affinity of bifunctional molecules for their elected substrates, and both halves of the FP peptides proved amenable to such fine-tuning. Indeed, it is of extreme importance to balance the binding affinities of both compounds[18]. To prevent the undesired hook effect, the two compounds must bind effectively to the heterobifunctional

molecule. This can be adjusted by the versatility of Fibril Paint peptides.

Fibril Paint peptides offer a great opportunity in the development of disease-modifying compound for neurodegenerative disease. Although their molecular signature still remains elusive, by systematic modification of FP1 we have gained insights about it. Importantly, we have described that that sequence of Fibril Paint peptides can be varied and adapted without compromising their functionality. Altogether, we have generated a class of peptides that can be the basis for the development of compounds targeting amyloid fibrils for diagnostics and therapy.

Author contributions

Conception JAP, FAD, TG, AF, SGDR
Design of the work JAP, FAD, SGDR
Acquisition JAP, FAD, KG, LML, SS, TG, GM
Analysis JAP, FAD, KG, LML, SGDR
Interpretation of data JAP, FAD, KG, LML, SGDR
Writing original draft JAP
Revision JAP, FAD, TG, AF, SGDR

Conflicts of interest

JAP, FAD, TG, GM, AF and SGDR are named as inventors in a patent (EP23194706, 'Peptides for the detection of amyloid fibril Aggregates') filed by Universiteit Utrecht Holding BV describing the peptides mentioned in this manuscript. The other authors declare no competing interests.

Data availability

Data for this article is provided as additional information document.

Acknowledgements

Measurements on the FIDA1 were done at the Protein Research Centre of Utrecht University. SGDR was supported by grants of the Campaign Team Huntington and Alzheimer Nederland (No. WE.03-2019-03). AF thanks The Minerva Center for Bio-Hybrid complex systems and the Saerree K. and Louis P. Fiedler Chair in Chemistry. SGDR is PIs of the gravitation consortium FLOW, funded by the Nederlands Minister of Education, Culture and Science.

References

(1) Hartl, F. U. Protein Misfolding Diseases. *Annual Review of Biochemistry* **2017**. DOI: 10.1146/annurev-biochem-061516-044518 (acccessed Apr 24).
(2) Knowles, T. P.; Vendruscolo, M.; Dobson, C. M. The amyloid state and its association with protein misfolding diseases. *Nature reviews: Molecular cell biology* **2014**, *15* (6), 384-396. DOI: 10.1038/nrm3810 (acccessed Jun).
(3) Chowdhury, S.; Chowdhury, N. S. Novel anti-amyloid-beta (Aβ) monoclonal antibody lecanemab for Alzheimer's disease: A systematic review. *Int J Immunopathol Pharmacol* **2023**, *37*, 3946320231209839. DOI: 10.1177/03946320231209839 From NLM.
(4) Cohen, S.; van Dyck, C. H.; Gee, M.; Doherty, T.; Kanekiyo, M.; Dhadda, S.; Li, D.; Hersch, S.; Irizarry, M.; Kramer, L. D. Lecanemab Clarity AD: Quality-of-Life Results from a Randomized, Double-Blind Phase 3 Trial in Early Alzheimer's Disease. *J Prev Alzheimers Dis* **2023**, *10* (4), 771-777. DOI: 10.14283/jpad.2023.123 From NLM.
(5) Van Dyck, C. H.; Swanson, C. J.; Aisen, P.; Bateman, R. J.; Chen, C.; Gee, M.; Kanekiyo, M.; Li, D.; Reyderman, L.; Cohen, S.; et al. Lecanemab in Early Alzheimer's Disease. *New England Journal of Medicine* **2023**, *388* (1), 9-21. DOI: 10.1056/nejmoa2212948.
(6) Agency, E. M. Refusal of the marketing authorisation for Leqembi (lecanemab). *European Medicines Agency (EMA)* **2024**.
(7) Garfagnini, T.; Ferrari, L.; Koopman, M. B.; Dekker, F. A.; Halters, S.; Van Kappel, E.; Mayer, G.; Bressler, S.; Maurice, M. M.; Rudiger, S. G. A peptide strategy for inhibiting different protein aggregation pathways. *Chemistry–A European Journal* **2024**, e202400080.
(8) Ferrari, L.; Stucchi, R.; Konstantoulea, K.; van de Kamp, G.; Kos, R.; Geerts, W. J. C.; van Bezouwen, L. S.; Förster, F. G.; Altelaar, M.; Hoogenraad, C. C.; et al. Arginine pi-stacking drives binding to fibrils of the Alzheimer protein Tau. *Nature communications* **2020**, *11* (1), 571-577. DOI: 10.1038/s41467-019-13745-7 (acccessed Jan 29).
(9) Aragonès Pedrola, J.; Dekker, F., A.; Garfagnini, T.; Mayer, G.; Koopman, M., B.; Bergmeijer, M.; Förster, F.; Hoozemans, J., J. M.; Jensen, H.; Friedler, A.; et al. Fibril Paint to detect Amyloids and determine Fibril Length. *BioRxiv* **2023**. DOI: https://doi.org/10.1101/2023.10.13.562220.
(10) Weber, P. J. A., Bader, J. E., Folkers, G., and Beck-Sickinger, A. G. A fast and inexpensive method for N-terminal fluorescein-labeling of peptides. *bioorganic & medicinal chemistry letters* **1998**, *8*, 597-600.
(11) Fleming, P. J.; Fleming, K. G. HullRad: Fast Calculations of Folded and Disordered Protein and Nucleic Acid Hydrodynamic Properties. *Biophysical Journal* **2018**, *114* (4), 856-869. DOI: 10.1016/j.bpj.2018.01.002 (acccessed 2024-06-17T11:46:26).
(12) Madsen, A. V. M.-G., Oscar; Pedersen, Lasse E.; Skovgaard, Kerstin; Kristensen, Peter; Goletz, Steffen. Immobilization-Free Binding and Affinity Characterization of Higher Order Bispecific Antibody Complexes Using Size-Based Microfluidics. *Analytical Chemistry* **2022**, *94*, 13652−13658.
(13) Spillantini, M. G.; Goedert, M. Tau pathology and neurodegeneration. *The Lancet.Neurology* **2013**, *12* (6), 609-622. DOI: 10.1016/S1474-4422(13)70090-5 (acccessed Jun).
(14) Andrew, S. E.; Goldberg, Y. P.; Kremer, B.; Telenius, H.; Theilmann, J.; Adam, S.; Starr, E.; Squitieri, F.; Lin, B.; Kalchman, M. A. The relationship between trinucleotide (CAG) repeat length and clinical features of Huntington's disease. *Nature genetics* **1993**, *4* (4), 398-403. DOI: 10.1038/ng0893-398 (acccessed Aug).
(15) Scheepstra, M.; Hekking, K. F. W.; van Hijfte, L.; Folmer, R. H. A. Bivalent Ligands for Protein Degradation in Drug Discovery. *Computational and structural biotechnology journal* **2019**, *17*, 160-176. DOI: 10.1016/j.csbj.2019.01.006 (acccessed Jan 25).
(16) Wang, Y.; Jiang, X.; Feng, F.; Liu, W.; Sun, H. Degradation of proteins by PROTACs and other strategies. *Acta pharmaceutica Sinica.B* **2020**, *10* (2), 207-238. DOI: 10.1016/j.apsb.2019.08.001 (acccessed Feb).
(17) Hanzl, A.; Winter, G. E. Targeted protein degradation: current and future challenges. *Current opinion in chemical biology* **2020**, *56*, 35-41. DOI: S1367-5931(19)30139-5 [pii] (acccessed Jun).
(18) Kuemper, S.; Cairns, A. G.; Birchall, K.; Yao, Z.; Large, J. M. Targeted protein degradation in CNS disorders: a promising route to novel therapeutics? *Frontiers in Molecular Neuroscience* **2024**, *17*. DOI: 10.3389/fnmol.2024.1370509 (acccessed 2024-08-22T10:47:23).
(19) Lin, Z. G., Benjamin A. ; Lv, Dongwen. Bifunctional Peptide Nanofibrils for Targeted Protein Degradation. *Angewandte Chemie (International ed in English)* **2024**, *63* (e202316581).

(20) Dekker, F. A., Aragonès Pedrola, J., Poza-Rodríguez, A., Mayer, G., Singh, S., Heesink, G., Claessens M. M. A. E., Friedler, A., Rüdiger, S. G. D. Fibril Paint targets amyloid fibrils for ubiquitination *BioRxiv* **2024**. DOI: https://doi.org/10.1101/2024.08.27.609886.
(21) Ji, C. H.; Kim, H. Y.; Lee, M. J.; Heo, A. J.; Park, D. Y.; Lim, S.; Shin, S.; Yang, W. S.; Jung, C. A.; Kim, K. Y.; et al. The AUTOTAC chemical biology platform for targeted protein degradation via the autophagy-lysosome system. *Nature communications* **2022**, *13* (1), 904-904. DOI: 10.1038/s41467-022-28520-4 (acccessed Feb 16).
(22) Takahashi, D.; Moriyama, J.; Nakamura, T.; Miki, E.; Takahashi, E.; Sato, A.; Akaike, T.; Itto-Nakama, K.; Arimoto, H. AUTACs: Cargo-Specific Degraders Using Selective Autophagy. *Molecular cell* **2019**, *76* (5), 797-810.e710. DOI: S1097-2765(19)30694-X [pii] (acccessed Dec 5).
(23) Pei, J.; Pan, X.; Wang, A.; Shuai, W.; Bu, F.; Tang, P.; Zhang, S.; Zhang, Y.; Wang, G.; Ouyang, L. Developing potent LC3-targeting AUTAC tools for protein degradation with selective autophagy. *Chemical communications (Cambridge, England)* **2021**, *57* (97), 13194-13197. DOI: 10.1039/d1cc04661f (acccessed Dec 7).
(24) Cassidy, K.; Zhao, H. Redefining the Scope of Targeted Protein Degradation: Translational Opportunities in Hijacking the Autophagy-Lysosome Pathway. *Biochemistry* **2021**. DOI: 10.1021/acs.biochem.1c00330 (acccessed Sep 27).